

1 **Distinct ionospheric long-term trends in Antarctica due to the** 2 **Weddell Sea Anomaly**

3 Marayén Canales¹, Trinidad Duran², Manuel Bravo³, Andriy Zalizovski⁴, Alberto Foppiano³

4 ¹ Departamento de Geofísica, Universidad de Concepción, Concepción, 4070386, Chile

5 ² Departamento de Física, Universidad Nacional del Sur, Bahía Blanca, 8000, Argentina

6 ³ Centro de Instrumentación Científica, Universidad Adventista de Chile, Chillán, 3780000, Chile

7 ⁴ Institute of Radio Astronomy, National Academy of Sciences of Ukraine, Kharkiv, 61002, Ukraine

8 *Correspondence to:* Marayén Canales (mcanales2019@udec.cl)

9 **Abstract.** The Weddell Sea Anomaly (WSA), a summer ionospheric anomaly over the eastern Antarctic Peninsula, was first
10 observed in 1958 and is characterized by a nighttime peak in electron concentration, unlike the typical daytime peak. There
11 are some works that examine long-term trends at ionospheric stations in the WSA region but they do not do a seasonal-diurnal
12 analysis that is vital for differentiating the periods of the anomaly. This study investigates the seasonal-diurnal variation of the
13 long-term trend in the F2 layer critical frequency (foF2) at ionospheric stations located within the WSA region: Vernadsky
14 (Argentine Island; 65.1°S, 64.2°W) and Port Stanley (51.6°S, 57.9°W), both with long-term foF2 data. Data from Vernadsky
15 (1960-2023) and Port Stanley (1960-2019) were analyzed alongside data from Syowa (69.0°S; 39.6°E) and Mawson (67.6°S;
16 62.9°E), two stations outside the WSA influence. The analysis reveals distinct seasonal and diurnal trends. For Vernadsky,
17 negative foF2 trends (-0.02 MHz/year) are observed during summer nights, coinciding with the WSA's presence. Port Stanley
18 shows similar trends but with a secondary nighttime maximum. The WSA's influence on Vernadsky is more pronounced, with
19 Port Stanley exhibiting a weaker, mid-latitude summer evening anomaly. In contrast, Syowa and Mawson show different
20 trends, with Syowa without a clear trend pattern, and Mawson showing negative trends throughout the year. The study
21 concludes that the WSA significantly affects Vernadsky and, to a lesser extent, Port Stanley. The findings highlight regional
22 variations in ionospheric behavior and contribute to the ongoing discussion on global ionospheric trends, suggesting that local
23 phenomena like the WSA can modulate these trends.



24 **1 Introduction**

25 The Weddell Sea Anomaly (WSA) is a summer abnormality in the ionosphere over the eastern Antarctic Peninsula,
26 characterized by maximum electron concentration occurring during nighttime hours instead of the typical daytime peak. The
27 anomaly was first observed by Bellchambers and Piggott (1958) at the Halley Bay ionosonde (75.5°S; 26.6°W) in Antarctica,
28 located along the coast of the Weddell Sea. More recently, Total Electron Concentration (TEC) determined from satellite
29 measurements has shown this anomaly over the geographical region of 55°S to 75°S latitude and 80°W to 30°W longitude
30 (Zakharenkova et al., 2017).

31 We detected two ionosondes located in the WSA region with foF2 (F2 layer critical frequency) data records extensive enough
32 to analyze long-term trends linked to the anthropogenic activity: Argentine Island, also called Vernadsky (65.1°S, 64.2°W)
33 and Port Stanley (51.6°S, 57.9°W) located on the northern edge of the WSA. These trends have been of interest since a
34 pioneering study in 1989 suggesting that the long-term increase of greenhouse gases concentration due to anthropogenic
35 activity, particularly carbon dioxide, would produce a global cooling in the upper atmosphere in conjunction with the global
36 warming in the troposphere (Roble and Dickinson, 1989; Rishbeth, 1990). Since then, long-term changes in the upper
37 atmosphere, and particularly in the ionosphere, have become a significant topic in global change research with many results
38 already published as can be appreciated in the review works by Lastovicka and different co-authors (Lastovicka et al., 2012,
39 2014; Lastovicka, 2017, 2021a). Among these studies, we highlight those including the analysis of ionospheric stations located
40 within the WSA region.

41 The first study reporting trends at Port Stanley is that by Upadhyay and Mahajan (1998). Considering the period 1957-1990
42 and noon time hours they obtained an hmF2 (peak height of the F2 layer) trend of -0.33 km/year and a foF2 trend of -0.004
43 MHz/year. A year later, Jarvis et al. (1998) analyzed hmF2 at Argentine Island and Port Stanley along the period 1957-1995.
44 The trends obtained in this work, which are mostly negative, vary with month and time of day at both sites. They interpreted
45 these results either as a constant decrease in altitude combined with a decreasing thermospheric wind effect or as a constant
46 decrease in altitude which is altitude-dependent. Both interpretations left inconsistencies when the results from the two sites
47 are compared at that time, but the estimated long-term hmF2 decrease along the period considered was of a similar order of
48 magnitude to that which has been predicted to result in the thermosphere from anthropogenic greenhouse gas increase. There
49 is no mention of the WSA, but this is expected since the anomaly is seen in foF2 daily variation, and not in hmF2. It is worth
50 mentioning that Alfonsi et al. (2001) tried to analyze Halley Bay trend, but after detecting errors in foF2 data series in the
51 period 1957-1990 it was discarded from the study.

52 Some of these stations have been included in later studies, such as Bremer et al. (2012), which conducted a global analysis
53 considering the Damboldt and Suessman database (Damboldt and Suessman, 2012) which covers up to ~2009, but again no
54 distinction is made about any anomalies and no markedly regional dependencies in trend values are found.

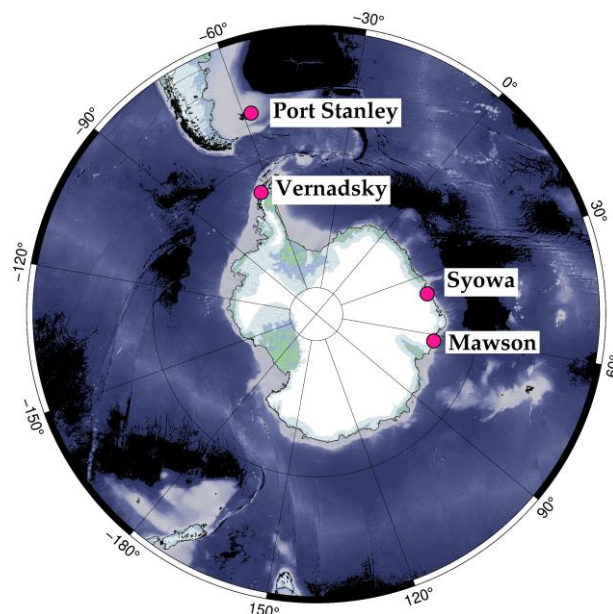
55 In the present study, the diurnal and seasonal variation of foF2 long-term trend is analyzed for stations within the Weddell Sea
56 anomaly region to contribute to the still controversial ionospheric trend topic and the detection and attribution of their forcings.



57 2 Data

58 The extensive dataset of monthly median foF2 from the Vernadsky ionospheric station, covering the period from 1996 to 2023.
59 Data spanning from 1960 to 1995 were sourced from the database made available by Damboldt and Suessmann (2012) in the
60 Australian Space Weather Forecasting Centre (www.sws.bom.gov.au). The Vernadsky Academician's station is a Ukrainian
61 research station in Antarctica, located at Marina Point on Galindez Island in the Argentine Island group of the Wilhelm
62 Archipelago (see Fig. 1). It was previously the Faraday Base (or F Base) of the United Kingdom, which transferred it to
63 Ukraine in 1996.

64 The Port Stanley dataset covering 1960 to October 2006 was obtained from the database made available by Damboldt and
65 Suessmann (2012), but it was supplemented with digisonde data from the Digital Ionogram Data Base (DIDBase,
66 <https://giro.uml.edu>), extending it until February 2019.



67
68 **Figure 1: Geographic locations of the ionospheric stations used in this work.**

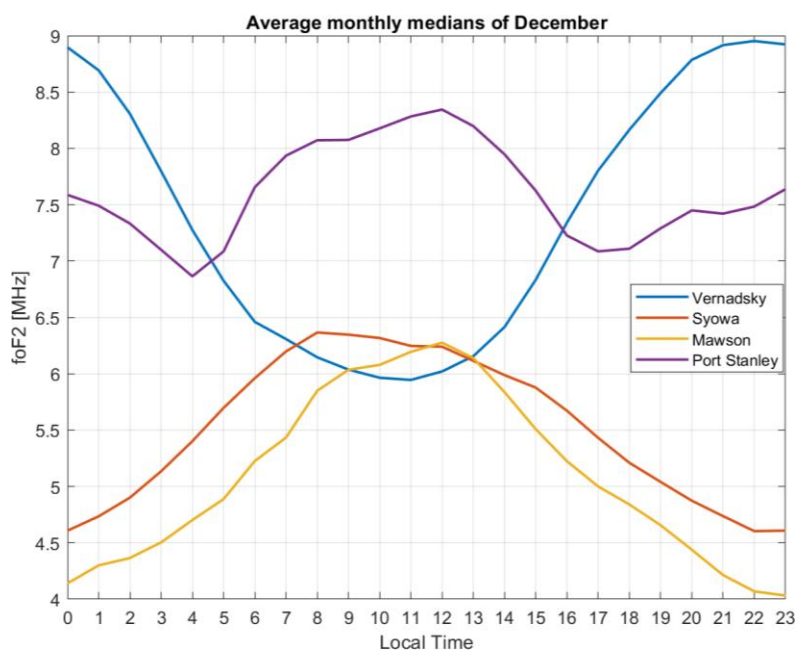
69 To investigate the potential impact of the Weddell Sea anomaly on Vernadsky and Port Stanley ionospheric stations, the
70 methodology will be applied to stations located outside the anomaly's influence zone. These stations are Syowa (69.0°S;
71 39.6°E) and Mawson (67.6°S; 62.9°E). Both datasets were also obtained from the database of Damboldt and Suessmann
72 (2012). The geophysical information of each station is presented in Table 1. The data used begins in 1960, as it was decided
73 to homogenize the study period to ensure a more consistent and precise comparison, avoiding the great solar maximum of
74 1958.



75 **Table 1: Geophysical information of ionospheric stations used in this work, according to the British Geological Survey**
 76 (<https://geomag.bgs.ac.uk/>).

Ionospheric station	Geographical coordinates	Geomagnetic coordinates	Period
Vernadsky	65.1°S; 64.2°W	51.4°S; 9.2°E	Jan 1960 - Dec 2023
Port Stanley	51.6°S; 57.9°W	40.0°S; 10.6°E	Jan 1960 - Oct 2006 + Nov 2006 - Feb 2019
Syowa	69.0°S; 39.6°E	66.6°S; 73.8°E	Jan 1960 - Dec 2023
Mawson	67.6°S; 62.9°E	70.6°S; 92.6°E	Jan 1960 - Dec 2023

77 Monthly median foF2 for each of the 24 daily hours were considered along the period January 1960-December 2023 of each
 78 station, except for Port Stanley which covers the period 1960-2019. The presence of the WSA becomes evident at Vernadsky
 79 when comparing its summer diurnal foF2 variations with Syowa and Mawson stations (see Fig. 2). However, Port Stanley is
 80 not completely affected by the WSA, but there is only a secondary maximum at night, or what is known as Mid-latitude
 81 Summer Evening Anomaly (MSEA) (Klimenko et al., 2015).



82
 83 **Figure 2: Diurnal variation in December of the average monthly medians of foF2 for the period between 1960 and 2023, for**
 84 **Vernadsky, Syowa and Mawson stations and between 1960 and 2019 for Port Stanley station.**



85 It is important to note that the data for Port Stanley come from two different sources: most of the records up to 2006 were
86 obtained using an ionosonde, while from that date onwards they began to be collected using a digisonde. When comparing the
87 data for the same years, a satisfactory agreement was observed between both sources, which led to the decision to use them
88 together. It is even more relevant to assess the quality of data from the Mawson and Syowa ionospheric stations, especially
89 considering that in some years complete records are not available. Possible deficiencies and missing data from these stations
90 are presumed to be due to their proximity to the auroral oval, a highly dynamic region where geomagnetic conditions can
91 significantly interfere with ionospheric measurements.

92 Monthly means of MgII (core-to-wing ratio of Mg II line), as an EUV solar proxy was used to filter out solar activity effect
93 from foF2. It was chosen in accordance with the recommendations provided by Laštovička (2021a, 2021b) and de Haro Barbas
94 et al. (2021). The MgII index is available from the University of Bremen at [http://www.iup.uni-](http://www.iup.uni-bremen.de/UVSAT/datasets/mgii)
95 [bremen.de/UVSAT/datasets/mgii](http://www.iup.uni-bremen.de/UVSAT/datasets/mgii) (Viereck et al., 2004; Snow et al., 2014).

96 The geomagnetic activity index A_p was also considered as an additional parameter in the filtering process. Monthly values
97 were obtained from the Kyoto World Data Center for Geomagnetism at <https://wdc.kugi.kyoto-u.ac.jp/index.html>.

98

99 **3. Methodology**

100 Given that the foF2 trends we aim to detect are very subtle, it is essential to filter out all other regular or known variations in
101 this parameter. By analyzing each month and hour individually, we can eliminate the seasonal and diurnal components of foF2
102 variation. This approach assumes that the remaining variability is primarily due to solar and geomagnetic activity along with
103 random noise inherent in any real-time series. The effect of solar and geomagnetic activity on each of these data series was
104 filtered in the usual manner (e.g., Duran et al., 2023) by estimating the residuals ($foF2gs$) through a multiple regression
105 between foF2 and MgII (as a proxy for solar activity) and A_p , as follows:

$$106 \quad foF2gs = foF2exp - (A * MgII^2 + B * MgII + C * A_p + D) \quad (1)$$

107 where $foF2exp$ represents the measured foF2 data, and A , B , C , and D are the least squares parameters of the regression between
108 $foF2exp$, the linear and quadratic terms of MgII, and the A_p index.

109 Finally, the $foF2$ linear trend, α , is estimated from:

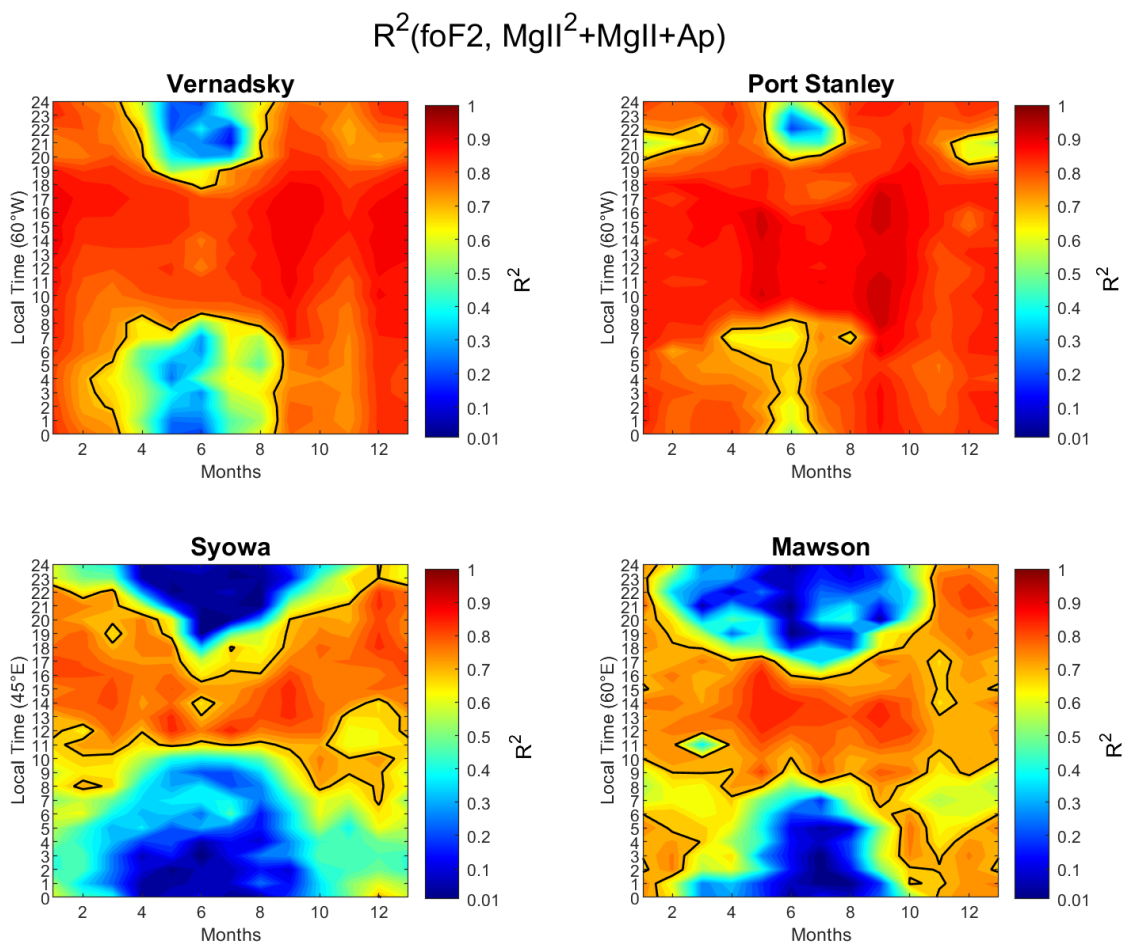
$$110 \quad foF2gs = \alpha t + \beta \quad (2)$$

111 where α in MHz/year and β in MHz are the least squares parameters of the linear regression between foF2 and time t in year.

112

113 **4. Results and Discussion**

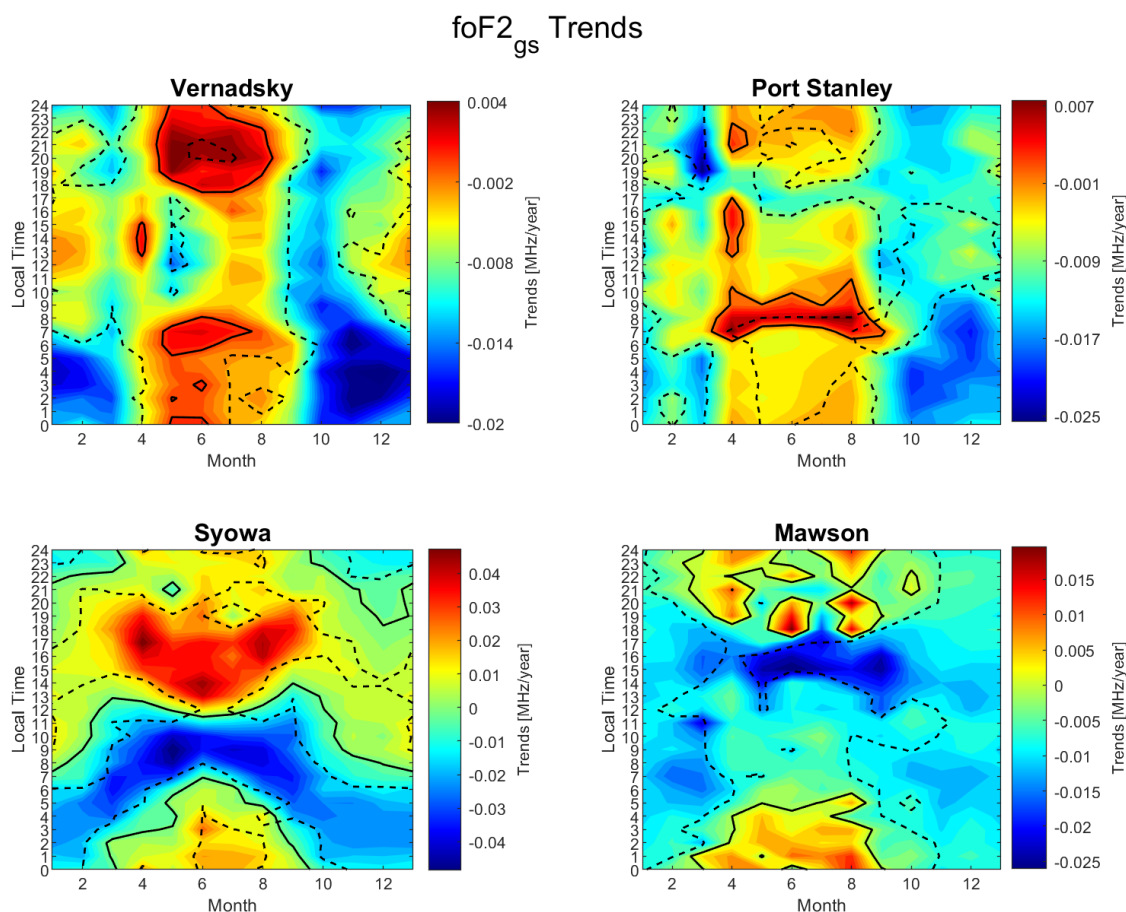
114 Figure 3 shows the values of the squared correlation coefficient, r^2 , between MgII, A_p , and foF2 indicating the fraction of foF2
115 monthly median variance explained by MgII index and A_p through equation (1) along the period 1960-2023, except for Port
116 Stanley, which covers the period 1960-2019.



117

118 **Figure 3: Seasonal-diurnal variation of squared correlation coefficient (r^2) for: (a) Vernadsky, (b) Port Stanley, d) Syowa, and (c)**
119 **Mawson. Solid black line: $r^2=0.75$**

120 Figure 3 illustrates a strong solar and geomagnetic dependence at Vernadsky during all hours in the summer, but only during
121 daylight hours (08:00-19:00 LT) for the rest of the year. This is likely due to the presence of the WSA in the summer months.
122 Port Stanley exhibits this strong dependence during almost all hours and across all seasons. This is due to its location at a lower
123 latitude compared to the rest of the stations. A similar pattern to Vernadsky is observed at Mawson, although weaker
124 correlations are observed during summer nights. In contrast, Syowa shows strong dependencies only during daylight hours
125 and dusk, with almost null correlation during the period between 23:00 and 08:00 LT in winter months.
126 Trends are then calculated for all hours across all years included in the study following the equation (2). The results are
127 displayed in Figure 4.



128

129 **Figure 4: Seasonal-diurnal variation of the foF₂ linear trend for: (a) Vernadsky, (b) Port Stanley, (c) Syowa, and (d) Mawson. Solid**
130 **black line is $\alpha=0$. Dashed black line is α with 95% significance.**

131 Figure 4 shows negative trends (extreme values of -0.02 MHz/year) for Vernadsky in the intervals where the explained variance
132 was significant, i.e., during all hours between end of September and December and at nighttime hours from January to March.
133 Also a small positive trend during winter between 20:00 and 21:00 LT is observed. Similar negative trends are observed at
134 Port Stanley at the same hours and months. Syowa and Mawson display opposite trends to each other. While Syowa shows
135 positive trends (+0.04 MHz/year) during the intervals of significant explained variance, negative trends (-0.02 MHz/year) are
136 observed for Mawson at the same hours.

137 The negative trends observed at the Vernadsky station coincide with the months and hours when the Weddell Sea anomaly is
138 present. The physical phenomenon responsible for these trends during these intervals is likely the same as the one affecting
139 Port Stanley. This can be inferred from the fact that Port Stanley exhibits a secondary maximum during the night (see Fig. 2).



140 Such a pattern is not observed at the Syowa and Mawson stations, which, despite their proximity (23° longitude apart), show
141 significantly different trends from each other.

142 Regarding the Weddell Sea anomaly and its impact on the ionosphere in this region, it is observed that it not only significantly
143 influences the Vernadsky station but also affects, albeit to a lesser extent, the Port Stanley station. As shown in Figure 2, during
144 the summer months, the foF2 parameter increases at night. The shape of the curve in this figure appears to combine the expected
145 trend in the absence of the anomaly (similar to the Mawson or Syowa curves) with a curve clearly influenced by the anomaly,
146 such as the Vernadsky curve. This behavior suggests that the Weddell Sea anomaly has a regionally differentiated effect,
147 modulating ionospheric characteristics based on the location of each station.

148 Moreover, since the WSA has been suggested to arise because the area is located farther away from the austral auroral zone
149 than locations at other longitude sectors along the same latitude (Richards et al., 2017 and 2018), the WSA may also depend
150 on the long term trend of the auroral zone itself. Indeed, perusal of the long term changes of the geomagnetic parameters in
151 the southern hemisphere using the International Geomagnetic Reference Field (IGRF20,
152 <https://www.ngdc.noaa.gov/geomag/calculators/magcalc.shtml>) shows that the austral auroral zone does move away from
153 middle latitudes at the American longitude sector between 1960 and 2024. So much so that the inclination of the magnetic
154 field at the WSA is almost stationary (in contrast to Concepción and Tucumán as seen in Foppiano et al., 1999) although the
155 total intensity of the field does decrease. This latter fact is related to the westward movement of the SAMA during the same
156 time interval.

157 In the case of Port Stanley, trends around -0.003 MHz/year are observed during the winter months between 10:00 and 14:00
158 LT, similar to the trends reported by Upadhyay and Mahajan (1998), who calculated a trend of -0.004 MHz/year for the period
159 from 1957 to 1990 during the same hours. However, between October and February, the trends calculated in this study are
160 lower than -0.005 MHz/year, reaching as low as -0.015 MHz/year in October (Fig. 4).

161 According to Danilov and Mikhailov (2001), using a third-degree polynomial on sunspot number to model foF2, the hourly
162 average trends for Vernadsky are negative throughout the day, which is consistent with the trends observed in this study, but
163 with different amplitudes (approximately half of the maximum value at 04:00 LT). When comparing Port Stanley, we again
164 find that the average hourly trends are negative for all hours, which is consistent with the trends in this study, but with double
165 the maximum values. On the other hand, when comparing the trends at 04:00 LT, neither Port Stanley nor Vernadsky show
166 differences in trends during the WSA months.

167 Syowa, according to model 1 of Alfonsi et al. (2001), shows negative trends in the monthly averages during the summer
168 months and positive trends during the winter, but with greater amplitude compared to this study. Model 1 consists in using
169 ITU-R global model to model foF2 and filter external forcings not linked to the greenhouse gas increase, which is a reason for
170 the difference in the trend absolute values between this study and Alfonsi et al. (2001). Specifically, in this study, between
171 23:00 and 07:00 LT, positive trends were found during the winter and negative trends during the summer. Then, between 08:00
172 and 13:00 LT, these trends reverse between winter and summer, and between 14:00 and 22:00 LT, they are positive throughout



173 the year. These same trends (model 1) for Mawson are negative throughout the year, consistent with this study, but with greater
174 amplitudes. During daylight hours, the trends are negative year-round, while at night, the trends in winter are close to zero.
175 The possibility of using time series only up to 2005 was evaluated, not only to maintain a single data source for Port Stanley,
176 but also because of solar minima that occurred after 2008, which could influence the trend results (Cnossen and Franzke.,
177 2014), obtaining similar results.

178 When comparing trends with those from other mid-latitude stations in South America, Foppiano et al. (1999) analyzed foF2
179 time series from the Concepción ionospheric station (36.8°S, 73°W) for the period 1958–1994. They found consistently
180 negative trends between 08:00 and 19:00 LT throughout the year. However, between 00:00 and 07:00 LT, the trends were
181 close to zero or positive, except during the summer months. Meanwhile, Jarvis et al. (1998), studying the trends (1957–1995)
182 in hmF2 at the Argentine Islands and Port Stanley, observed seasonal and diurnal variations. They reported predominantly
183 negative trends at Port Stanley, while smaller trends were noted at the Argentine Islands.

184 Several trend studies have been conducted on stations in the Southern Hemisphere. For example, Sharan & Kumar (2021) and
185 Duran et al. (2023) analyzed foF2 data at 00 and 12 LT from Australian ionospheric stations. In Sharan & Kumar (2021), foF2
186 data from Hobart, Canberra, and Christchurch (1947–2006) were examined. Their results revealed more significant trends at
187 midday (12 LT), with negative trends associated with F10.7 solar flux and small, insignificant positive trends linked to Rz.
188 They concluded that foF2 decreased by 0.1–0.4 MHz over five solar cycles, likely due to increased CO₂ in the troposphere
189 cooling the upper atmosphere. For its part, Duran et al. (2023) analyzed foF2 data from mid-to-low latitude stations up to 2022,
190 focusing on seasonal and diurnal variability. Their findings show overall negative trends, with the most significant declines
191 observed around the equinox. Weaker or slightly positive trends were seen in December–February and June–August, while
192 the diurnal pattern showed the strongest negative values during the day and the weakest at night.

193 To compare the experimental foF2 trend values with those from models assessing anthropogenic forcing effects, the results of
194 Solomon et al. (2018) are considered. They carried out simulations using the Whole Atmosphere Community Climate Model-
195 eXtended to investigate anthropogenic global changes across the entire atmosphere, including the thermosphere and
196 ionosphere, and identified CO₂ as the primary driver of temperature changes. For their simulations, they applied a CO₂
197 increase of 16 ppmv per decade, which led to a 1.2% reduction in peak electron density (NmF2). In this work, we find a foF2
198 maximum reduction of 3.5% per decade for Vernadsky and Port Stanley during months and hours of WSA. foF2 maximum
199 reductions of 10% and 6% were found for Syowa and Mawson, respectively, during other months and hours. All of these
200 percentages are much higher than those calculated in the literature (see De Haro Barbas & Elias, 2020; De Haro Barbas et al.,
201 2021; Duran et al., 2023).

202 The same long-term trend analysis has been performed but using F30 instead of MgII as an EUV solar proxy, as suggested by
203 recent studies (Laštovička and Burešová, 2023; Laštovička, 2024), however, the results (figure not shown) do not show
204 significant differences with those done with MgII.



205 **5. Conclusion**

206 The seasonal-diurnal variation of the long-term foF2 trend for stations within the Weddell Sea anomaly region is analyzed to
207 contribute to the still controversial issue of the ionospheric trend. The WSA is shown to significantly impact ionospheric
208 trends, particularly at Vernadsky, where negative trends are observed during periods when the WSA is active. This effect is
209 also detected in Port Stanley, although to a lesser extent, showing only a secondary maximum during the evening. These trends
210 seem to be consistent with the long-term apparent movement of the WSA relative to the austral auroral zone, which moves
211 poleward during the studied time interval due to the decreasing of the total intensity of the magnetic field over the area.

212 The trends in foF2 show seasonal-diurnal variations, with negative trends at Vernadsky and Port Stanley during specific hours
213 and months where the WSA is present. In contrast, Syowa and Mawson stations, in longitude sectors outside the WSA region,
214 do not show the same seasonal-diurnal behavior of the trends.

215 The results are consistent with some earlier studies, though the observed trend magnitudes differ. For example, trends at Port
216 Stanley match previous studies in terms of negative values, but with differing amplitudes. The study also aligns with findings
217 from other Southern Hemisphere stations which report negative trends in foF2 at various latitudes.

218 Other studies suggest a 1.2% reduction in NmF2 due to CO₂-driven temperature changes. This study found foF2 maximum
219 reductions values much larger than the literature at all stations. Particularly, Vernadsky and Port Stanley show the same
220 maximum reductions values at WSA months. Overall, the study underscores the complex interplay between solar,
221 geomagnetic, and regional factors in shaping ionospheric trends, with specific attention to the regional effects of the WSA.

222 **Author contribution**

223 MC: Formal analysis, data curation, writing – original draft preparation, validation. TD: Formal analysis, data curation, writing
224 – original draft preparation. MB: Conceptualization, methodology, writing – original draft preparation. AZ: Data mining. AF:
225 Supervision, writing – original draft preparation.

226 **Competing interests**

227 The authors declare that they have no conflict of interest.

228 **Acknowledgments**

229 We thank Ana G. Elias for her collaboration in the discussion and partial analysis of the results obtained. This work was
230 supported by the Universidad Adventista de Chile, Regular Project number 204. The authors are thanks to the Antarctic



231 Geospace and ATmosphere reseArch (AGATA) Scientific Research Programme. M. Bravo acknowledges to
232 ANID/FONDECYT Regular 1211144.



233 **References**

- 234 Alfonsi, L., De Franceschi, G., Perrone, L.: Long term trend in the high latitude ionosphere, *Phy & Chem. Earth, C*, 26, 303-
235 307, doi:10.1016/S1464-1917(01)00003-4, 2001.
- 236 Bellchambers, W. H. and Piggott, W. R.: Ionospheric measurements made at Halley Bay, *Nature*, 1596-1597, 1958.
- 237 Bremer, J., Damboldt, T., Mielich, J., and Suessmann, P.: Compar-ing long-term trends in the ionospheric F2-region with two
238 dif-ferent methods, *J. Atmos. Sol.-Terr. Phys.*, 77, 174–185, 2012.
- 239 Cnossen, I. & Franzke, C.: The role of the Sun in long-term change in the F2 peak ionosphere: New insights from EEMD and
240 numerical modeling, *J. Geophys. Res.*, 119, 8610–8623, doi:10.1002/2014JA020048, 2014.
- 241 Damboldt T. and Suessmann P.: Consolidated Database of Worldwide Measured Monthly Medians of Ionospheric
242 Characteristics foF2 and M(3000)F2. INAG (Ionosonde Network Advisory Group) Bulletin 73,
243 https://www.ursi.org/files/CommissionWebsites/INAG/web-73/2012/damboldt_consolidated_database.pdf, 2012.
- 244 de Haro Barbás, B.F., Elias, A.G., Venchiarutti, J.V., Fagre, M., Zossi, B.S., Tan Jun, G. & Medina, F.D.: MgII as a Solar
245 Proxy to Filter F2-Region Ionospheric Parameters. *Pure Appl. Geophys.* 178, 4605–4618 . doi:10.1007/s00024-021-02884-y,
246 2021.
- 247 Danilov, A. D. and Mikhailov, A. V.: F2-layer parameters long-term trends at the Argentine Islands and Port Stanley stations,
248 *Ann. Geophys.*, 19, 341–349, doi:10.5194/angeo-19-341-2001, 2001.
- 249 de Haro Barbás, B.F., Elias, A.G: Effect of the Inclusion of Solar Cycle 24 in the Calculation of foF2 Long-Term Trend for
250 Two Japanese Ionospheric Stations. *Pure Appl. Geophys.* 177, 1071–1078, doi:10.1007/s00024-019-02307-z, 2020
- 251 de Haro Barbás, B.F., Elias, A.G., Venchiarutti, J.V. et al: MgII as a Solar Proxy to Filter F2-Region Ionospheric Parameters.
252 *Pure Appl. Geophys.* 178, 4605–4618, doi:10.1007/s00024-021-02884-y, 2021
- 253 Duran, T., Melendi, Y., Zossi, B.S., De Haro Barbás, B.F., Buezas, F.S., Juan, A., and Elias, A.G.: Contribution to ionospheric
254 F2 region long-term trend studies through seasonal and diurnal pattern analysis, *Global Planet. Change*, 229, 104249,
255 doi:10.1016/j.gloplacha.2023.104249, 2023
- 256 Foppiano, A.J, Cid, L., and Jara, V.: Ionospheric long-term trends for South American mid-latitudes, *J. Atmos. Sol.-Terr.*
257 *Phys.*, 61, 9, 717-723, doi:10.1016/S1364-6826(99)00025-5, 1999.
- 258 Jarvis, M. J., Jenkins, B., and Rodgers, G. A.: Southern hemisphere observations of a long-term decrease in F region altitude
259 and thermospheric wind providing possible evidence for global thermospheric cooling, *J. Geophys. Res.*, 103(A9), 20775–
260 20787, doi:10.1029/98JA01629, 1998.
- 261 Klimenko, M.V., Klimenko, V. V., Ratovsky, K.G., Zakharenkova, I.E., Yasyukevich, Yu.V., Korenkova, N.A., Cherniak,
262 I.V., and Mylnikova, A.A.: Mid-latitude Summer Evening Anomaly (MSEA) in F2 layer electron density and Total Electron
263 Content at solar minimum, *Adv. Space Res.*, 56, 1951–1960, 2015.
- 264 Laštovička, J.: A review of recent progress in trends in the upper atmosphere. *J. Atmos. Sol.-Terr. Phys.*, 163, 2–13,
265 doi:10.1016/j.jastp.2017.03.009, 2017.



- 266 Lastovicka, J.: Long-Term Trends in the Upper Atmosphere, in Upper Atmosphere Dynamics and Energetics; Wang, W.,
267 Zhang, Y., Paxton, L.J., Eds.; American Geophysical Union: (Washington D.C) USA, 325–344, 2021a.
- 268 Laštovička, J.: What is the optimum solar proxy for long-term ionospheric investigations?, *Adv. Space Res.*, 67, 1, 2-8,
269 doi:10.1016/j.asr.2020.07.025, 2021b.
- 270 Laštovička, J.: Dependence of long-term trends in foF2 at middle latitudes on different solar activity proxies, *Adv. Space Res.*,
271 73, 1, 685-689, doi:10.1016/j.asr.2023.09.047, 2024
- 272 Laštovička, J., Beig, G., Marsh, D.R.: Response of the mesosphere-thermosphere-ionosphere system to global change-
273 CAWSES-II contribution. *Prog. Earth Planet. Sci.*, 1, 21, doi:10.1186/s40645-014-0021-6, 2014.
- 274 Laštovička, J., & Burešová, D. Relationships between foF2 and various solar activity proxies. *Space Weather*, 21,
275 e2022SW003359, doi:10.1029/2022SW003359, 2023
- 276 Laštovička, J., Solomon, S., Qian, L.: Trends in the Neutral and Ionized Upper Atmosphere. *Space Sci. Rev.*, 168, 113–145,
277 doi:10.1007/s11214-011-9799-3, 2012.
- 278 Richards, P. G., Meier, R. R., Chen, S., & Dandenault, P.: Investigation of the causes of the longitudinal and solar cycle
279 variation of the electron density in the Bering Sea and Weddell Sea anomalies. *Journal of Geophysical Research: Space
280 Physics*, 123, 7825–7842. 10.1029/2018JA025413, 2018.
- 281 Richards, P. G., Meier R. R., Chen S.-P., Drob D. P. and Dandenault P.: Investigation of the causes of the longitudinal variation
282 of the electron density in the Weddell Sea Anomaly, *J. Geophys. Res. Space Physics*, 122, 6562–6583,
283 doi:10.1002/2016JA023565, 2017.
- 284 Rishbeth, H.: A greenhouse effect in the ionosphere? *Planet. Space Sci.*, 38, 945–948, 1990.
- 285 Roble, R.G.; Dickinson, R.E.: How will changes in carbon dioxide and methane modify the mean structure of the mesosphere
286 and thermosphere? *Geophys. Res. Lett.*, 16, 1441–1444, 1989.
- 287 Sharan, A. & Kumar, S.: Long-term trends of the F2-region at mid-latitudes in the Southern Hemisphere, *J. Atmos. Solar-Terr.
288 Phys.*, 220, 105683, doi:10.1016/j.jastp.2021.105683, 2021
- 289 Snow, M., Weber, M., Machol, J., Viereck, R., Richard, R.: Comparison of Magnesium II core-to-wing ratio observations
290 during solar minimum 23/24, *J. Space Weather Space Clim.*, 4, A04, doi: 10.1051/swsc/2014001, 2014.
- 291 Solomon, S. C., Liu, H. L., Marsh, D. R., McNerney, J. M., Qian, L., & Vitt, F. M.: Whole atmosphere simulation of
292 anthropogenic climate change. *Geophys Res Lett*, 45, 1567–1576, doi:10.1002/2017GL076950, 2018.
- 293 Upadhyay, H.O., Mahajan, K.K.: Atmospheric greenhouse effect and ionospheric trends, *Geophys. Res. Lett.*, 25, 3375-3378,
294 doi:10.1029/98GL02503, 1998.
- 295 Viereck, R. A., Floyd, L. E., Crane, P. C., Woods, T. N., Knapp, B. G., Rottman, G., Weber, M., Puga, L. C., and DeLand,
296 M. T.: A composite Mg II index spanning from 1978 to 2003, *Space Weather*, 2, S10005, doi:10.1029/2004SW000084, 2004
- 297 Zakharenkova, I., Cherniak, I., and Shagimuratov, I.: Observations of the Weddell Sea Anomaly in the ground-based and
298 space-borne TEC measurements, *J. Atmos. Sol.-Terr. Phys.*, 161, 105-117, doi:10.1016/j.jastp.2017.06.014, 2017.